Journal of Nuclear Materials 392 (2009) 386–395

Contents lists available at ScienceDirect

Journal of Nuclear Materials

journal homepage: www.elsevier.com/locate/jnucmat

Kinetics of self-interstitial cluster aggregation near dislocations and their influence on hardening

Ming Wen [a,*], Akiyuki Takahashi [b], Nasr M. Ghoniem [a]

[a] Department of Mechanical and Aerospace Engineering, University of California, 420 Westwood Plaza, Ste. 48-121, Los Angeles, CA 90095, USA
[b] Department of Mechanical Engineering, Tokyo University of Science, Chiba, Japan

ARTICLE INFO

Article history:
Received 7 March 2008
Accepted 19 October 2008

ABSTRACT

Kinetic Monte Carlo (KMC) computer simulations are performed to determine the kinetics of SIA cluster 'clouds' in the vicinity of edge dislocations. The simulations include elastic interactions amongst SIA clusters, and between clusters and dislocations. Results of KMC simulations that describe the formation of 'SIA clouds' during neutron irradiation of bcc Fe and the corresponding evolution kinetics are presented, and the size and spatial distribution of SIA clusters in the cloud region are studied for a variety of neutron displacement damage dose levels. We then investigate the collective spatio-temporal dynamics of SIA clusters in the presence of internal elastic fields generated by static and mobile dislocations. The main features of the investigations are: (1) determination of the kinetics and spatial extent of defect clouds near static dislocations; (2) assessment of the influence of localized patches of SIA clouds on the pinning–depinning motion of dislocations in irradiated materials; and (3) estimation of the radiation hardening effects of SIA clusters. The critical stress to unlock dislocations from self-interstitial atom (SIA) cluster atmospheres and the reduced dislocation mobility associated with cluster drag by gliding dislocations are determined.

1. Introduction and background

Self-interstitial atom (SIA) clusters that readily form in a variety of irradiated bcc, fcc and hcp metals are usually treated as nanoscale prismatic dislocation loops. These clusters nucleate on the periphery of collision cascades and subsequently perform fast thermally-activated one-dimensional (1D) motion [1]. The motion and interaction of SIA clusters have drastic effects on the physical and mechanical properties of irradiated materials, most notably their influence on void swelling [2] and radiation hardening [3,4]. The interaction between a single SIA cluster and other clusters, stacking fault tetrahedra, or single dislocations has been extensively studied by atomistic simulations [5–7]. Nevertheless, some of the most important phenomena associated with SIA clusters, such as their spatial segregation into heterogeneous aggregates and their agglomeration around dislocations in 'clouds' similar to Cottrell atmospheres [3,8], have not yet been investigated because of the size limitations of atomistic simulations. These phenomena are the result of the collective behavior of a large number of SIA clusters, and as such one must rely on statistical mechanics or equivalent computer simulation techniques to resolve the spatio-temporal dynamics of SIA cluster ensembles. Analytical calculations [4] as well as kinetic Monte Carlo (KMC) simulations [8] have shown that the motion and interactions of SIA clusters lead to the formation of dislocation loop rafts and the decoration of dislocations by SIA clusters. However, the kinetics of SIA cluster cloud evolution, the collective interaction between SIA clusters and dislocations, and the spatial heterogeneity of SIA aggregates have not yet been explored.

The formation of SIA cluster rafts and clouds around dislocations have significant impact on the onset of plastic yield and subsequent hardening as a result of dislocation interaction with spatially segregated SIA clusters. When the applied stress is increased above a critical value, grown-in dislocations that are trapped by SIA cluster clouds may drag some of these clusters along, and thus freed dislocations would have reduced mobility. Drag on dislocations by SIA clusters, and dislocation interaction with immobile vacancy clusters or with other dislocations determine the rate of work-hardening in the post-yield deformation regime. In irradiated materials, the presence of irradiation-induced defects alters the plastic deformation behavior significantly, and it is therefore important to investigate the role played by SIA cluster ensembles.

Radiation hardening has been described by the change in the critical resolved shear stress (CRSS) due to an array of defects in the two limiting cases of 'strong' or 'weak' obstacles. If the obstacles are strong, the change in CRSS is expressed as $\Delta\tau = \alpha\mu b/l$, where α is a parameter representing the obstacle strength, μ is the shear modulus, b is the magnitude of the Burgers vector and l is the average inter-obstacle distance. On the basis of Orowan's work for strong obstacles [9], Seeger [10] developed a hardening

* Corresponding author. Tel.: +1 310 825 8917; fax: +1 310 206 4830.
E-mail address: wenm@seas.ucla.edu (M. Wen).

0022-3115/$ - see front matter © 2009 Published by Elsevier B.V.
doi:10.1016/j.jnucmat.2008.10.029

model in which vacancy clusters are referred to as 'depleted zones'. An alternative obstacle-controlled hardening model was developed for weak obstacles by Friedel–Kroupa–Hirsch (FKH) [11,12]. In this limiting case, the increase of the critical shear stress by a random array of obstacles of diameter d and volume density N is given by $\Delta\tau = \frac{1}{8}\mu b d N^{2/3}$. Correlation with experiments in both these limiting cases is qualitative at best, and has only been examined for the onset of plastic flow, i.e. at the yield point. Although, these analytical models have been used to explain experimental observations, they suffer from uncertainties associated with describing the obstacle strength. In addition, they do not provide any information on post-yield deformation, including the observed yield drop during tensile testing of irradiated materials. In analogy with the Cottrell hardening model due to an atmosphere of impurities [13] around dislocations, Singh, Trinkaus and Foreman proposed the mechanism of cascade induced source hardening (CISH) [3,4]. Their approach provides a rational explanation for the observed occurrence of yield drop in irradiated fcc metals. Singh et al. [3] proposed that the irradiation-induced increase in the yield stress is a consequence of trapping the majority of F–R sources by 'defect clouds', and their subsequent release when the applied stress exceeds a critical value. The issue of dislocation pinning by radiation-induced SIA clusters and the subsequent depinning of dislocations upon application of an external stress field is central to the understanding of radiation hardening. The physics of SIA cluster 'cloud' formation and the interaction between dislocations and such clouds require more detailed computer simulations.

The objective of the present study is to investigate the kinetics of SIA cluster cloud evolution in the presence of internal elastic fields generated by dislocations, and the subsequent influence of the formation of such clouds on dislocation motion under applied stress. The effects of dislocation pinning by SIA clouds on radiation hardening will also be assessed. The present investigation is based on the model developed in Ref. [8], with the following new features: (1) the kinetics and spatial extent of defect clouds near static dislocations; (2) the interaction between mobile dislocations and glissile SIA clusters; and (3) the hardening effects due to SIA clusters. First, we present results of KMC simulations that describe the formation of SIA clouds during neutron irradiation of bcc Fe and the corresponding evolution kinetics in Section 2.2. We report on the size and spatial distribution of SIA clusters in the cloud region as function of the neutron displacement damage dose. The results are then used in Section 3 as input to parametric dislocation dynamics (PDD) simulations aimed at determination of the influence of SIA clouds on dislocation motion and on the critical stress for dislocation unlocking from SIA defect atmospheres. Conclusions are finally presented in Section 4.

2. Kinetics of SIA cluster cloud evolution

2.1. Computer simulation method

To study the spatial distribution of SIA clouds around dislocations and the evolution kinetics of such clouds in bcc Fe, we utilize KMC simulation methodology of Wen et al. [8]. Elastic interactions between irradiation-induced SIA clusters and dislocations are incorporated in the present KMC simulations of SIA defect cloud evolution. The interaction between SIA clusters is calculated by linear elasticity theory, where the cluster is treated as a circular infinitesimal prismatic dislocation loop with its Burgers vector in a closed-packed $\langle 1\,1\,1\rangle$-direction normal to its habit plane. The relationship between the loop radius, R, and the number of self-interstitial atoms in the cluster, N, is $N = \sqrt{3}\pi R^2/a^2$, where α = 0.2867 nm is the lattice constant of iron. Although, small irradiation-induced interstitial clusters made of parallel $\langle 1\,1\,0\rangle$ dumbbells are found to be stable in bcc iron [14], larger clusters adopt either the $\langle 1\,1\,1\rangle$ or the $\langle 1\,0\,0\rangle$ orientation [15], as observed in experiments [16]. Interstitial loops of the $\langle 1\,0\,0\rangle$-type are regarded as nearly immobile, based on experimental evidence and the fact that migration energies larger than 2.5 eV have been reported [15]. Therefore, the present investigation will focus on interstitial clusters as the dominant type in clouds and rafts in bcc Fe. The numerical method developed by Ghoniem and Sun [17] is employed to evaluate the interaction between small defect clusters and dislocations. Since SI A clusters are glissile, they perform 1D random motion in the slip direction parallel to the Burgers vector of the loop. An SIA cluster may change its moving direction by a thermally-activated Burgers vector change. However, as the cluster size increases, thermally-activated re-orientation from one Burgers vector to another becomes increasingly more difficult. Re-orientation of the Burgers vector can still take place when one accounts for the elastic interaction energy between clusters, or between clusters and dislocations [8].

To analyze the spatial distribution of SIA clusters in the vicinity of dislocations and the kinetics of cloud build-up, we first consider a KMC model that involves the interaction between an edge dislocation and SIA clusters. A computational box of $300a \times 300a \times 300a$ is used and the simulation box edges are oriented parallel to the cubic axes. An edge dislocation with $\mathbf{b} = a/2[\bar{1}\,1\,1]$ lying on a $(1\,0\,1)$ plane is inserted in the simulation box. The simulation box represents an isolated region around a straight edge dislocation in an infinite medium, where the stress field is due to the dislocation and the surrounding SIA clusters. A periodic boundary condition is imposed on the motion of SIA clusters in and out of the simulation box to preserve a net zero flux for existing SIA clusters.

2.2. Formation of SIA clouds near edge dislocations

KMC simulations require detailed information on defect production due to displacement cascades. Only a very small fraction of defects produced in collision cascades can escape recombination reactions within the cascade volume and migrate freely through the lattice [18]. We therefore used the initial defect configurations produced by 100 keV displacement cascades, obtained from MD simulations of Bacon et al. [18] as input, and performed separate KMC simulations to obtain the number and configuration of SIA clusters that escape the immediate cascade region and migrate long distances in the matrix. The conversion of the number of Frenkel pairs N_F produced by a single displacement cascade to damage dose P (in units of dpa) is given by $P = N_F/N_t$, where N_t is the total number of atoms in the simulation volume. KMC simulation results of a single 100 keV displacement cascade results in 36 SIA clusters with size ranging from 1 to 35 SIAs. The fraction of SIAs in large clusters (containing more than 14 SIAs) is 54%. The size distribution of large clusters resulting from KMC simulations of single cascades are then used as input in the present study. Specifically, in the present KMC simulations, 60% of all interstitial clusters initially introduced into the simulation box contain 14-SIAs, 20% contain 21-SIAs, and the rest contain 35-SIAs. We introduce this size distribution of SIA clusters because TEM observations of are not capable of differentiating smaller clusters [4].

In post-irradiation experiments, the material is first irradiated in an unstressed condition to a particular damage dose level that corresponds to a specific density of SIA clusters. To simulate irradiation conditions, we assume here that the dislocation is rigid and fixed in the simulation volume, and a sequence of 100 keV displacement cascades are continuously introduced into the simulation box at a fixed dose rate of 5×10^{-6} dpa/s. For every single cascade, the number and size distribution of clusters are assumed to be identical, while they are randomly placed in the simulation box.

Diffusion of interstitial clusters is governed by a generalized size-dependent Arrhenius law, developed by Osetsky et al. [5] to describe the 1D diffusional transport behaviors of SIA clusters

$$\omega = \omega_0 n^{-s} \exp\left(-\frac{E_m}{k_B T}\right), \quad (1)$$

where E_m is the average effective activation energy, n is the number of SIAs in the cluster, and ω_0 is a pre-exponential factor. The value of E_m was found to be close to that of an individual crowdion. For clusters containing up to 91 SIAs in iron, it is estimated that $E_m = 0.023 \pm 0.003$ eV for $\langle 1\,1\,1\rangle$ clusters [5]. By fitting to the results of numerous simulations, the following parameter values for Fe were found to describe the MD data very well, and are used in our KMC simulations: $\omega_0 = 6.1 \times 10^{12}\ s^{-1}$, and $S = 0.66$. Rotation to other close-packed glide directions is also governed by an Arrhenius law, with an assumed attempt frequency is the same as ω_0, and an assumed activation energy of 0.05 eV per crowdion. This linear dependence of the energy barrier for rotation on cluster size is adopted on the basis of MD simulations confirming that the motion of SIA clusters is the result of the motion of individual $\langle 1\,1\,1\rangle$ crowdions [5], and that the re-orientation may occur in a one-by-one fashion [19]. For small interstitial clusters, such as 2- or 3-SIAs clusters, the activation energy for rotation predicted by atomistic simulations [20] is higher than the value given by the simple 0.05 eV per crowdion relationship used in the present study. However, actual values for the rotation energy barriers are as yet unknown for the large clusters used in our simulations because the time-scale involved is prohibitive for MD simulations. For large clusters involved in the present study, the current estimated value of 0.05 eV per crowdion will result in the energies for rotation bigger than 0.7 eV, and is sufficient to preserve the preferential 1D motion of large interstitial clusters [8]. It is noted that the elastic interaction energy between SIA clusters and dislocations at a close range, or between SIA clusters themselves when they are within a few atomic distances from one another is sufficiently strong that clusters re-orient regardless of the exact value of the activation barrier.

The presence of internal stress fields, for example, dislocations and SIA clusters, would further enhance the 3D nature of SIA cluster transport. The possibility of the Burgers vector rotation may increase in the presence of the elastic interaction between clusters, and/or between clusters and dislocations. We performed additional simulations to demonstrate that cluster rotation is a prerequisite to the formation of dislocation decorations. Fig. 1 shows KMC simulation results of the microstructures in bcc Fe with an initial number of 400 SIA clusters distributed in the simulation box at 300 K with an energy barrier for rotation of 0.2 eV/crowdion. The simulation results indicate that dislocation decoration is negligible for a relatively small amount of irradiation-induced damages if interstitial clusters perform pure 1D motion. Simulations with an energy barrier of 1 eV/crowdion produced similar results to those of Fig. 1. However, experimental results [21] show that even at a very low damage dose, 0.0001 dpa, a clear increase in the yield stress is observed, from an unirradiated value of 138–160 MPa after irradiation. This suggests that dislocation decoration has already started building up at very low damage doses. In order to achieve a certain amount of decoration, SIA clusters must be able to change their orientation with lower energy barriers than energetics would suggest for thermally-activated spontaneous processes.

We performed KMC simulations for the evolution of an SIA cloud around an edge dislocation in pure iron irradiated at 300 K up to a displacement dose of 2.6×10^{-3} dpa. A sequence of 100 keV displacement cascades with the previously described size distribution was introduced randomly into the simulation box at a constant rate of 5×10^{-6} dpa. When an extremely mobile 1D migrating interstitial cluster passes through the neighborhood of a pre-existing dislocation, it feels the influence of the dislocations' strain field. The overall mobility and spatial distribution of SIA clusters are significantly changed as a result of dislocation–cluster interactions. With irradiation damage building up, a significant fraction of initially glissile clusters were found to be attracted to the dislocation forming a 'Λ' – shaped cloud. In effect, these clusters re-orient themselves by rotation of their Burgers vectors to respond to the elastic field of the dislocation. Fig. 2(a)–(d) shows the time evolution of the cloud build-up process on the tensile side of an edge dislocation in bcc Fe irradiated to 2.6×10^{-3} dpa at 300 K. The stress field of the dislocation, aided by cluster mutual elastic interactions, renders most of the clusters virtually immobile in the vicinity of the edge dislocation. At higher displacement damage doses, the percentage of SIA clusters trapped in the region of attractive elastic interaction is not as high as that at low doses, as the screening effects of existing defects increases, and SIA accumulation in the trapping region approaches saturation.

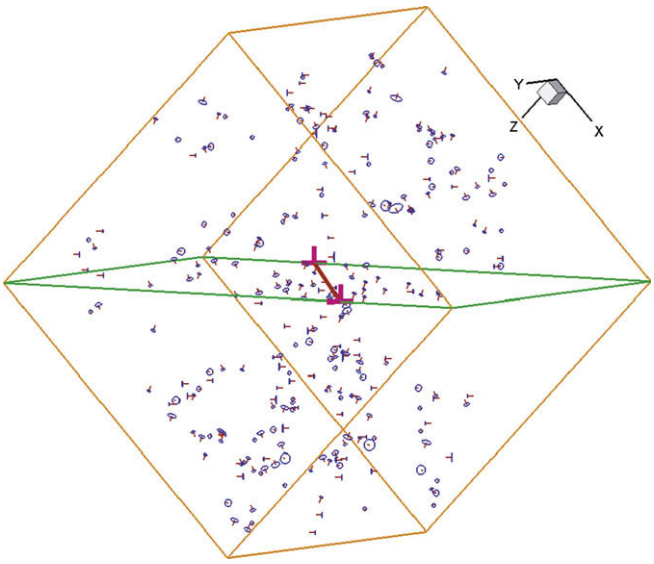

Fig. 1. KMC simulation result of microstructure in bcc Fe irradiated at 300 K with an initial number of 400 SIA clusters and a rotation energy barrier of 0.2 eV/crowdion.

To give a clear view of the structure of the cloud, we use lighter color for SIA clusters outside the SIA cloud and highlight those that were trapped in the cloud region in Fig. 2. Even at low damage doses, for example at 0.0002 dpa as shown in Fig. 2(a), SIA clusters are already trapped in the region of positive dilatational strain in the vicinity of the edge dislocation, where the elastic interaction between the dislocation and the SIAs is attractive. The clusters form two wings that are 30° with respect to the normal direction of the slip plane. It is observed that most of the trapped defect clusters have Burgers vectors that are parallel to that of the edge dislocation. In view of the initial random distribution of SIA clusters' Burgers vectors, the present results confirm that SIA clusters near dislocations rotate their Burgers vectors in response to the influence of the strain field of the edge dislocation. As the displacement damage dose increases, the two wings consisting of SIA clusters continue to grow, and become more packed and prominent because of additional cluster trapping. With further agglomeration of SIA clusters in extended cluster wings, trapped clusters start to precipitate in between the two wings and lead to the eventual disappearance of the distinct and separate wings, as shown in Fig. 2(c and d) shows that at 0.0026 dpa, a wedge-shaped SIA cluster 'cloud' has been fully developed along the dislocation line. The formation of a Cottrell-like atmosphere in the vicinity of

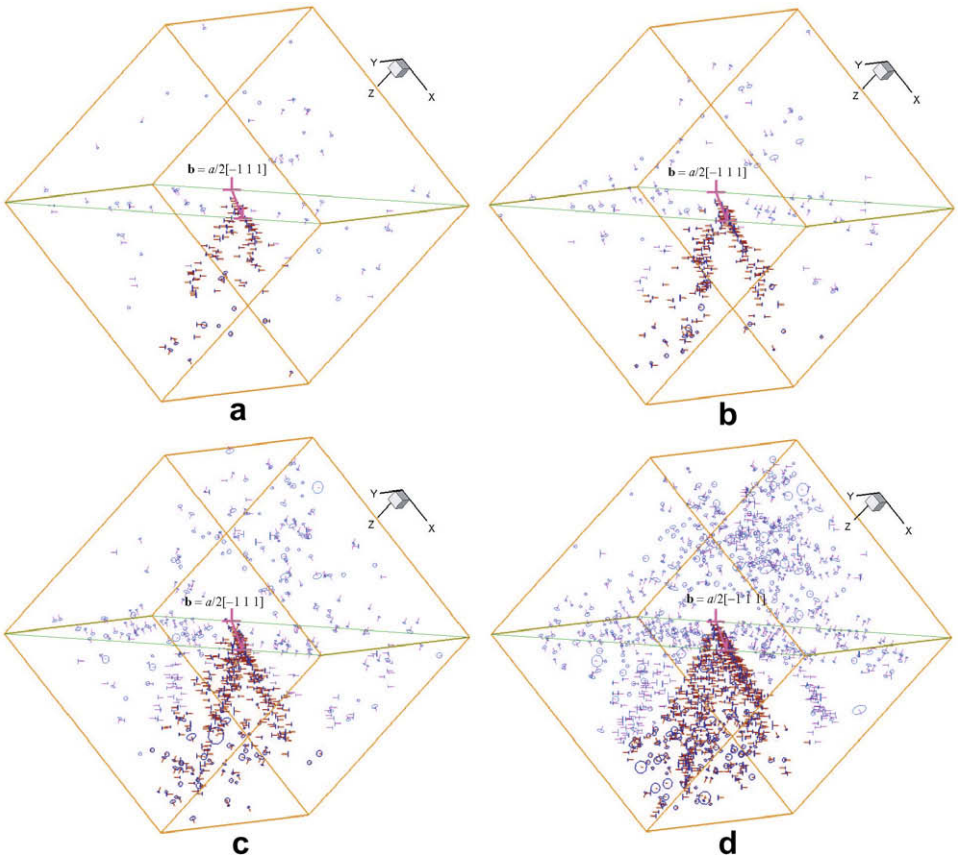

Fig. 2. SI A cluster cloud evolution on the tensile side of an edge dislocation in bcc Fe irradiated at 300 K to a displacement dose level of (a) 2×10^{-4} dpa, (b) 4×10^{-4} dpa, (c) 0.001 dpa, and (d) 0.0026 dpa, respectively. The edge dislocation has a Burgers vector $\mathbf{b} = a/2[\bar{1}\,1\,1]$. Each SIA cluster is represented by a small circle corresponding to its size with a line segments pointing along its Burgers vector direction. SIA clusters that are trapped in the cloud region are highlighted.

dislocations has been investigated experimentally, theoretically and numerically [3,4,8]. However, the characteristic arrangement and morphology of SIA clouds (which are important for studying microstructure evolution and the corresponding effects plastic deformation) have never been examined. The present simulations indicate that at low damage dose, a 'Λ' – shaped wing structure made up of SIA clusters is formed first, and wedge-shaped clouds are finally developed when SIA clusters are immobilized in the space between the wings.

In the trapping region close to the slip plane of the edge dislocation, the Burgers vectors of most clusters are parallel to the edge dislocation's Burgers vector. In the outer region, however, the orientational distribution of the Burgers vectors is almost random. This implies that as the cloud evolves, the attractive stress field of the edge dislocation is gradually shielded by the defect clusters in the cloud. New cluster trapping takes place now ahead of the existing configuration resulting from the elastic interaction between clusters themselves and their mutual immobilization. Because the dominant mechanism for cluster trapping is cluster–cluster interaction instead of dislocation–cluster interaction, metastable immobile complexes consisting of SIA clusters with non-parallel Burgers vectors may form. Furthermore, we can expect that at a certain stage, SIA cluster trapping will stop, and that the defect cluster concentration in the trapping region will reach saturation. This saturation behavior is a consequence of two effects: (1) the build-up of the cloud near the edge dislocation, thus neutralizing its stress field, and (2) the evolution of damage in the matrix in between dislocations. In this work, damage is represented by sessile SIA clusters that are self-trapped in the matrix, but if one takes into account vacancy clusters as well, the saturation may be reached even at smaller dose. SIA loop coarsening may become significant and would eventually lead to the formation of dislocation walls, as pointed out by Trinkaus et al. [22].

3. The influence of SIA clouds on dislocation motion

The interaction between a dislocation and SIA clouds is investigated by the parametric dislocation dynamics (PDD) method, described elsewhere [23]. The stress field of dislocations is calculated by the fast sum method [17], while an analytical form due to Kroupa is utilized to calculate the stress of SIA clusters as infinitesimal dislocation loops [24]. In the following, we present results of dislocation dynamics simulations for the unpinning process of dislocations from their surrounding SIA cluster clouds. We first consider an isolated patch of SIA clusters, and then present estimates for the hardening effect due to SIA clouds trapping dislocations. We also present results for the interaction between SIA clusters and dislocations under applied stress in an effort to study the influence of SIA clusters on the effective mobility of dislocations in irradiated materials.

3.1. Pinning of dislocations by SIA clouds

The interaction between a glissile dislocation and a cloud of SIA clusters is important in two respects. First, one needs to estimate the degree of SIA source hardening at a given displacement damage dose by determining the critical stress necessary to pull a dislocation away from its cloud. Then, once the pinned dislocation pulls away from its cloud, it is interesting to determine the resistance

to its glide motion by pockets of cloud remnants that increase the effective back stress on the dislocation. We will investigate here the resistance of localized SIA clouds to dislocation glide motion, where we assess the influence of SIA cluster motion (i.e. sessile versus glissile clusters) on the effective mobility of dislocations. The magnitude of source hardening will also be estimated by PDD simulations.

Fig. 3 shows a typical volume used in the present simulations, of size: 1 μm × 1 μm × 200 nm. The *x*, *y* and *z* axes are along the $[\bar{1}\,\bar{2}\,1]$, $[\bar{1}\,1\,1]$ and $[\bar{1}\,0\,\bar{1}]$ directions, respectively. A straight edge dislocation with $[\bar{1}\,1\,1]$ Burgers vector is placed on the $(\bar{1}\,0\,\bar{1})$ slip plane. In order to remove any effects of boundary conditions, the two end points of the dislocation line are restricted to move only along the intersection lines of the slip plane and the two $(\bar{1}\,\bar{2}\,1)$ planes at the boundaries. Also, the directions of the tangent vectors of the end points are fixed to the $[\bar{1}\,\bar{2}\,1]$ direction, which is parallel to the tangent vector of the initial straight edge dislocation. It should be noted that only glide motion of dislocations is involved in the current study. SIA clouds obtained from previous KMC simulations are directly used as input into the simulation volume. For the sake of simplicity and in view of the formation of immobile complexes consisting of SIA clusters with non-parallel Burgers vectors in SIA clouds, all SIA clusters are assumed to be immobile in these simulations. We will later examine the effects of the simultaneous dynamic motion of the dislocation and SIA clusters in the cloud. The external shear stress is gradually increased by 1 MPa, and then a time-relaxation is performed for 2000 time steps to obtain an equilibrium shape of the dislocation. This process is repeated until the dislocation breaks away from the SIA cloud, and thus a critical value of the break-away shear stress is determined.

We first investigate the motion of a dislocation, locally decorated by an SIA cloud that is 110 nm along the dislocation line. The relative positions of the dislocation and the SIA cloud are directly obtained from previous KMC simulations. The simulations indicate that at low applied stress, the middle of the dislocation, which is decorated by the SIA cloud, cannot move while the rest of the dislocation glides on the slip plane. This behavior suggests that the SIA cloud has a pinning effect on the dislocation. Bowing out of the dislocation is extended by increasing the externally applied shear stress. The dislocation eventually breaks away from the SIA cloud when the applied shear stress reaches a critical value. The interaction between a dislocation and a pre-existing SIA cloud is also of interest, because the cloud may result of pinning of other mobile dislocations on nearby glide planes. Fig. 4 illustrates the relative positions of the dislocation and the SIA cloud as initial simulation conditions. The slip plane of the dislocation is selected at 20 nm and at 40 nm from the top of the SIA cloud. The slip plane at 40 nm from the top is very close to the bottom of the SIA cloud. The moving dislocation is initially free from any decorations, and

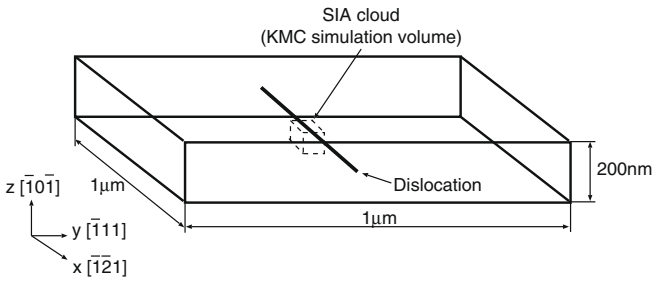

Fig. 3. Schematic of the volume used in PDD simulations of the interaction between a dislocation and an SIA cluster cloud. The dislocation is initially straight, and the SIA cloud is obtained from the results of separate KMC simulations.

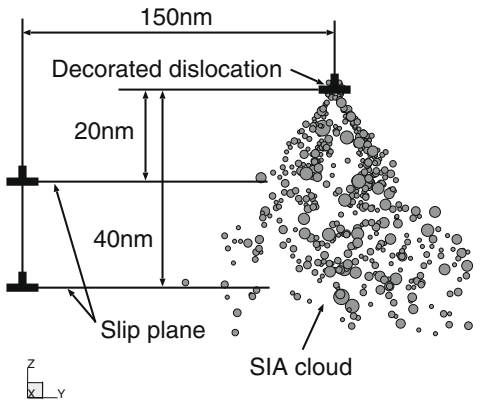

Fig. 4. Dislocation positions in PDD simulations of interactions between a dislocation and a pre-existing SIA cloud.

the distance between the initial dislocation position and the SIA cloud on the slip plane is taken to be 150 nm.

Fig. 5 shows the dependence of the critical shear stress on the irradiation dose for an SIA cloud formed at 2×10^{-4}, 4×10^{-4}, 10^{-3}, 2×10^{-3} and 2.6×10^{-3} dpa. In the figure, the critical shear stress for the decorated dislocation (i.e. $d = 0$) increases from 3 to 19 MPa as the irradiation damage dose increases from 2×10^{-4} to 2×10^{-3} dpa. The critical shear stress at 2×10^{-3} dpa is about six times larger than that at 2×10^{-4} dpa. Beyond that range, the critical shear stress begins to saturate because of the shielding effects of the cloud contents. The figure also illustrates the dependence of the critical shear stress on the displacement damage dose (i.e. the cloud content). The dependence of the critical shear stress on irradiation damage dose is similar in the three cases, but the position of the slip plane clearly changes the magnitude of the critical shear stress.

When the dislocation glides on the middle slip plane, the critical shear stress becomes smaller than that for the initially decorated dislocation. On the other hand, when the dislocation glides on the bottom slip plane, the critical shear stress again becomes larger. To gain a better understanding of the role of the SIA cloud on resisting the motion of dislocations gliding on various slip planes, we show in Fig. 6 a top view of dislocation configurations as it interacts with the cloud. When dislocations glide on slip planes at the bottom of clouds, they feel long-range repulsive

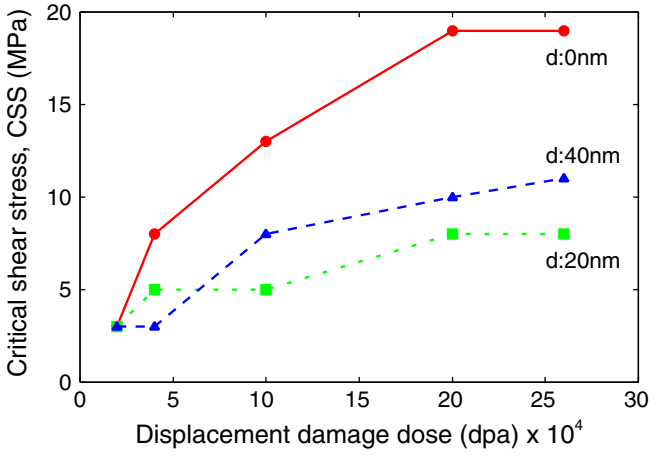

Fig. 5. Critical shear stress for cutting through a localized SIA cluster cloud. The critical shear stress of a dislocation decorated with an SIA cloud is also shown ($d = 0$).

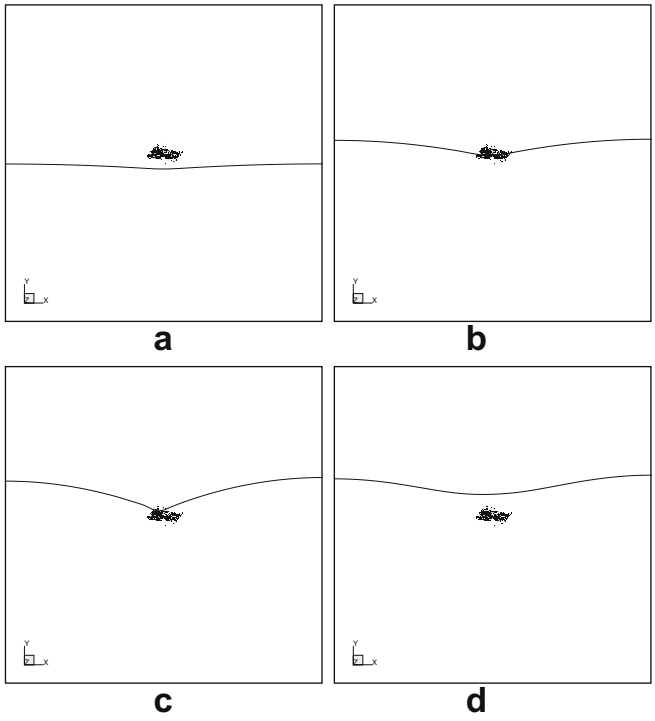

Fig. 6. Top view of dislocation configurations as it interacts with a pre-existing SIA cluster cloud on a slip plane 40 nm below the top of the cloud. (a) 2 MPa, (b) 4 MPa, (c) 10 MPa and (d) 11 MPa.

forces, and the dislocation starts to be bending before it physically meets the SIA cloud. Generally, SIA clusters prefer to be on the tension side of the dislocation, and are not likely to be on the compression side. A dislocation feels an attractive force from clusters on the tension side, and a repulsive force from clusters on the compression side. In the case of the middle slip plane, almost half of the SIA clusters are on the compression side, and the rest are on the tension side. Therefore, half of the clusters results in an attractive force, while the other half induces a repulsive force on the dislocation. These two types of forces partially cancel one another, and consequently, the pinning effect of the SIA cloud becomes weaker than that of the case of a cloud directly decorating the dislocation. On the other hand, in the case of the bottom slip plane, the majority of the clusters are on the compression side. The dislocation thus feels mainly a repulsive force, and thus the critical shear stress becomes larger than that in the case of the middle slip plane.

We consider now the process of full dynamic interaction between a moving dislocation and glissile SIA clusters in the cloud. Here, the equations of motion for the dislocation nodes and clusters have to be solved simultaneously. The results of this simulation are shown in Fig. 7 for the clouds at 10^{-3} dpa. The figure clearly shows that the SIA cloud works as a localized obstacle, which results in a pinning effect on the dislocation. As the dislocation approaches the cloud, SIA clusters are swept into various configurations, most of which are self-trapping. However, the dislocation succeeds in dragging a few SIA clusters along, as shown in the figure, which results in reduced dislocation mobility. It is thus reasonable to conclude that SIA clouds act as localized pinning obstacles, and that they also result in increasing the drag on further dislocation motion, and thus reduce dislocation mobility. It is noted that only a very small fraction of SIA clusters that are close to the slip plane of the dislocation in the cloud are dragged by the dislocation. It suggests that the development of the extensive SIA cloud is due to immobile complexes consisting of SIA clusters with non-parallel Burgers vectors that are formed in the cloud.

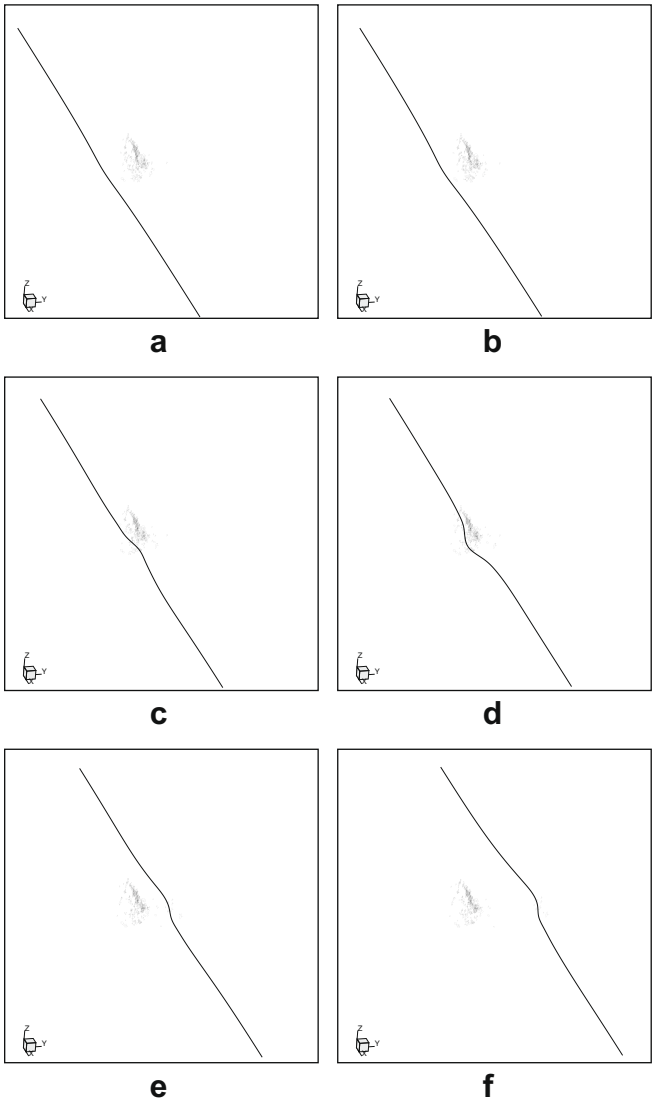

Fig. 7. Configurations of a moving dislocation and a dynamic SIA cloud during the interaction between the dislocation and cloud. The applied stress (in MPa) at each snapshot is: (a) 4; (b) 10;(c) 14; (d) 18; (e) 20 and (f) 26.

The majority of the SIA clusters in the cloud are held together by mutual cluster–cluster interactions.

3.2. Dislocation depinning and the influence of SIA clouds on hardening

The critical shear stress for dislocation unlocking from extensive decorations by SIA clouds is evaluated here, and this corresponds to the initiation of plastic yield under irradiation. To represent extensive decoration by SIA clouds, we constructed an array of localized SIA cluster clouds from separate KMC simulations along the dislocation line in order to decorate the entire dislocation. Fig. 8 shows the dislocation configurations during the break-away process from the SIA cluster clouds (i.e. source hardening) at 2.6×10^{-3} dpa. In this case, dislocation stops gliding on the slip plane due to the strong pinning by the SIA cloud. A small dislocation segment suddenly gets released from the cloud atmosphere (corresponding to a weak point in the cloud), and the entire dislocation then succeeds to unzip from the cloud. During the unzipping process of the dislocation line from the SIA cloud, all SIA clusters are assumed to be sessile. Fig. 9 shows the critical shear stress as a function of the neutron displacement dose for

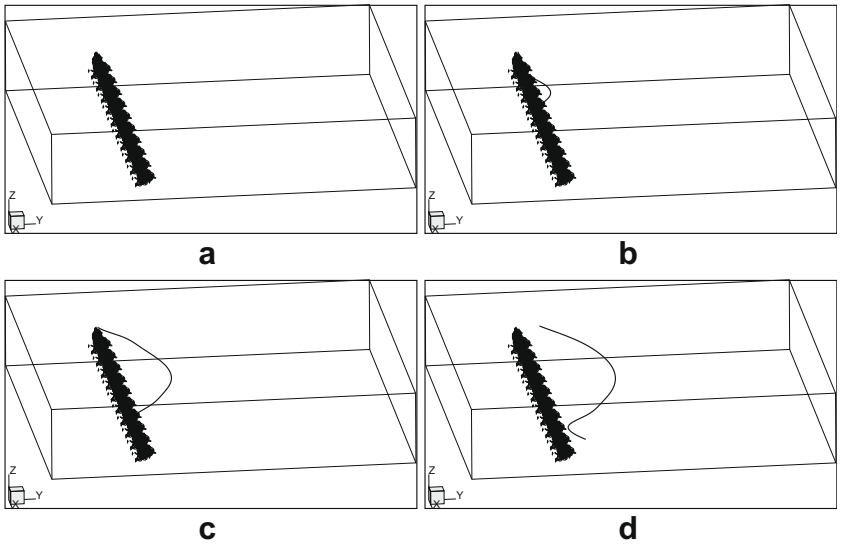

Fig. 8. Dislocation configurations as it breaks away from source hardening SIA clouds. (a) 76 MPa, (b) 80 MPa, (c) 84 MPa and (d) 86 MPa.

source hardening by SIA clusters. The critical shear stress (CSS) at 2×10^{-4} dpa is 32 MPa, and the stress increases gradually to 48 MPa at 4×10^{-4} dpa and about 72 MPa at 10^{-3} dpa. The CSS then increases slowly beyond 1×10^{-3} dpa with increasing dose, as seen in Fig. 9.

Eldrup et al. performed irradiation experiments on Fe in the high flux isotope reactor (HFIR) [21], and determined the stress–strain relationships in tension at a strain rate of $1.2 \times 10^{-3}\ s^{-1}$. Using a Taylor factor of 3.06 [25], we show in Fig. 10(a) comparison between their experiments and results of the present simulations. In the model used here, SIA clusters corresponding to a particular dose are introduced in the simulation volume and are allowed to diffuse one-dimensionally till they self-trap or aggregate around the dislocation in a cloud. Thus, one expects that the gradual build-up of SIA clouds in the experimental situation should result in weaker interactions because of recombination events that take place over time. Notwithstanding these limitations, the comparison between experiments and the current model should be taken as qualitative at best, and with these limitations borne in mind. At the low dose of 2×10^{-4} dpa, the measured value of radiation hardening (i.e. increase in yield stress) is lower than the experimental value indicating that the major contribution to the yield strength in the experiments may be due to dislocation–dislocation interactions and dislocation interaction with small vacancy clusters. On the other hand, the calculated values for the increase in the equivalent uniaxial tensile stress at 10^{-3}, 2×10^{-3} and 2.6×10^{-3} dpa are in qualitative agreement with experimental results, and thus it may be possible that SIA cluster hardening becomes dominant.

3.3. Motion of decorated dislocations

In this section, we consider the simultaneous motion of dislocations and SIA clusters. All SAI clusters are taken here to be mobile and interactive with the dislocation and amongst themselves. When a dislocation is released from the clouds that decorate it, the long-range elastic interaction between the dislocation and SIA clusters may tend to make some of the clusters that are close to the dislocation line glide along with the line. This may also reduce dislocation mobility [26]. MD simulations have demonstrated that interstitial loops can be dragged at extremely high speed by a gliding dislocation, and a model has been developed to describe the phenomenon of cluster drag [27]. The simulation setup is similar to

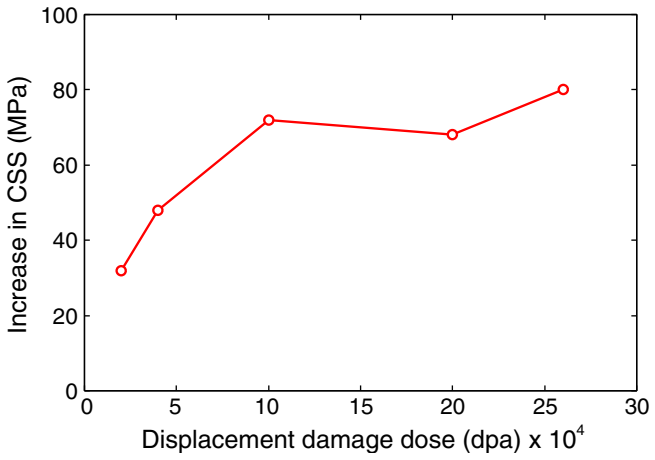

Fig. 9. Critical shear stress (CSS) as a function of neutron displacement damage dose due to dislocation source hardening by SIA clouds.

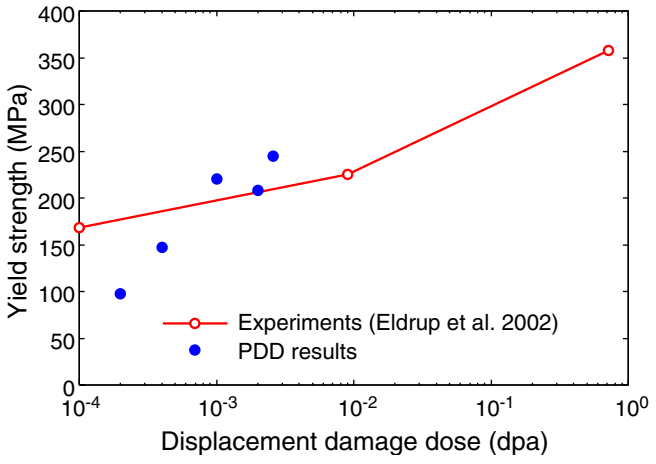

Fig. 10. Yield strength as a function of displacement damage dose. PDD simulation results are plotted with solid circles, and experimental results obtained by Eldrup et al. [23] are plotted as circles with connecting line.

that used in Section 3.2, and the localized SIA cluster clouds obtained from KMC simulations for bcc Fe irradiated to 0.001 dpa are utilized.

For simplicity, all SIA clusters are assumed to be rigid circular platelets and the analytical solution of the stress field of infinitesimal loops given by Kroupa [24] is utilized to calculate the force exerted on the dislocation line. The equation of motion for the center of a rigid SIA clusters can be written as

$$\frac{dx_i^{SIA}}{dt} = -\frac{M}{A}\int \frac{\partial \sigma_{jk}}{\partial x_i} b_j n_k dA, \tag{2}$$

where x_i^{SIA} is the center of the ith rigid SIA cluster, M is the mobility, L is the circumference of the SIA cluster, A is its area, b_j and n_k are, respectively, the Burgers vector and unit vector normal to the plane of the SIA cluster, and σ_{jk} is the stress tensor due to the dislocation and other SIA clusters. Here, the equations of motion for the dislocation nodes as well as the SIA clusters have to be solved simultaneously. The external shear stress is gradually increased by 1 MPa.

We first investigate the dynamics of an edge dislocation that is decorated by SIA clouds along the dislocation line in bcc iron irradiated to 0.001 dpa at 300 K. The initial relative positions of the dislocation and SIA clouds, as well as the nature of the SIA clusters (glissile or sessile) in the clouds are obtained from separate KMC simulations described in Section 2.2. We show in Fig. 11(a) series of snapshots of dislocation configurations as it interacts with the SIA cloud. Since some SIA clusters in the clouds are glissile and trapped in the cloud region only due to mutual cluster–cluster interaction, when the dislocation approaches the cloud, the long-range elastic interaction between the dislocation and SIA clusters may push some of the clusters out of the cloud region, as shown in Fig. 11(a) and (b). As a result of the elastic interaction between SIA clusters and the moving dislocation, some of the glissile clusters in the cloud region lying close to the glide plane of the dislocation are swept along the dislocation line, as the dislocation unzips from the cloud.

We consider now the dynamic interaction process between a moving edge dislocation and a fully mobile SIA cloud, i.e., all the SIA clusters in the cloud are assumed to be glissile. The results of this simulation are shown in Fig. 12. As soon as the dislocation moves, a small number of SIA clusters are pushed out of the cloud and stay at quasi-equilibrium positions at the perimeter of the cloud, as shown in Fig. 12(a and b), and the majority of the clusters in the cloud also adjust themselves by moving to new nearby equilibrium positions. As the applied stress increases, the edge dislocation is pulled out of the cloud with a number of SIA clusters dragged along. This process is similar to that of the previous case of an edge dislocation interacting with a decoration cloud containing some immobile SIA clusters. The two main differences are the critical unlocking stress for the dislocation detrapping from the cloud and the number of SIA clusters dragged by the released dislocation. The dislocation trapped in a fully mobile could is released from the atmosphere at a lower applied shear stress as compared to the previous case, as can be seen in the comparison between 11(b) and 12(b). The number of SIA clusters that is dragged by the moving edge dislocation in Fig. 12 is greater than that in Fig. 11, because the sessile complexes in the decoration cloud have a much stronger restraining force. As the applied shear stress increases, the unlocked dislocation moves faster. When the dislocation velocity reaches to a critical value, the forces exerted on SIA clusters are no longer strong enough to drag them along with the dislocation. As a result, these interstitial clusters are discarded by the moving dislocation. This scenario is indicated by the clusters distributed in the wake of the moving dislocation in both Figs. 11(d) and 12(d).

The effective or average dislocation mobility M is calculated by $v_{ave}/b\tau_{app}$, where wave is the average velocity of dislocation, b is

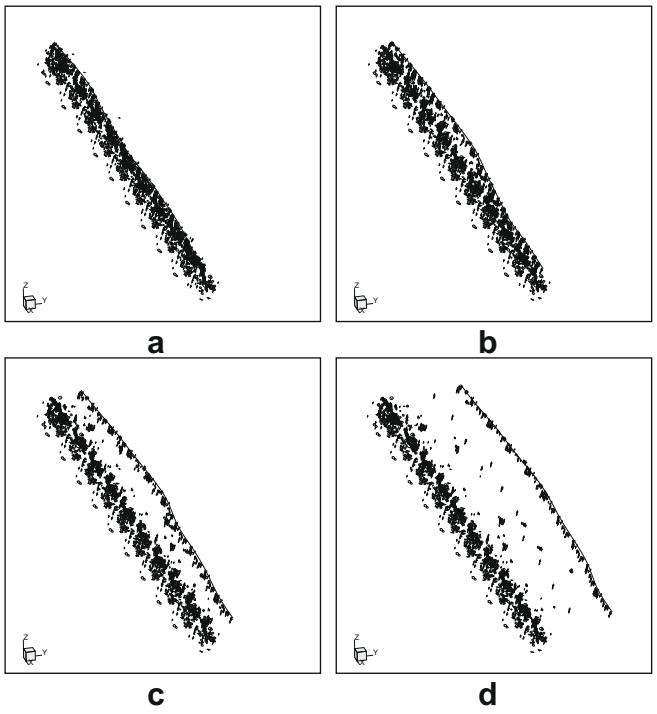

Fig. 11. Snap-shots of a moving edge dislocation and a decorating SIA cloud, namely a partially mobile cloud, during the release process of the dislocation from the SIA cloud in bcc iron irradiated to 0.001 dpa at 300 K. The applied resolved shear stress at each snapshot is: (a) 40 MPa, (b) 56 MPa, (c) 66 MPa, and (d) 80 MPa, respectively.

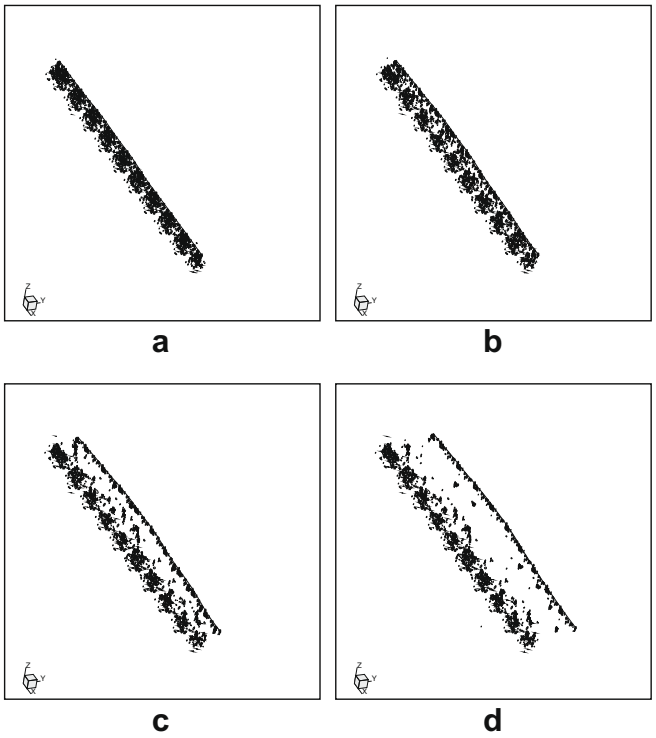

Fig. 12. Snap-shots of a moving edge dislocation and a fully mobile SIA cloud during the release process of the dislocation from the SIA cloud in bcc iron irradiated to 0.001 dpa at 300 K. The applied resolved shear stress at each snapshot is: (a) 30 MPa, (b) 48 MPa, (c) 64 MPa, and (d) 80 MPa, respectively.

the magnitude of Burgers vector and τ_{app} is the applied resolved shear stress. Fig. 13 shows the stress dependence of M/M_0, where the mobility is normalized to that of an unirradiated material (M_0). It is observed that the value of M has a rapid increase between 46–60 MPa for the interaction of the dislocation with a cloud containing some sessile clusters. On the other hand, the effective dislocation mobility increases gradually as a function of the applied stress for a cloud in which all SIA clusters are glissile. For the dislocation in both Figs. 11 and 12 the dislocation mobility is considerably reduced, compared with that of a dislocation in an unirradiated material, and eventually reaches to a saturation value that depends on the fraction of sessile clusters in the cloud.

4. Discussion and conclusions

The 1D motion of SIA clusters and the fact that they are associated with a polarized strain field engender unique characteristics to them, and result in several interesting phenomena [3,4,8]. The present study, which is based on two different simulation techniques: the KMC and the PDD methods, reveal more detailed aspects of SIA clusters in irradiated iron. Since these simulation methods are both based on the elastic theory of dislocations, they are limited primarily in their spatial resolution to dimensions greater than several interatomic distances. Nevertheless, these simulation methods provide good opportunities for studies of phenomena that involve ensembles of SIA clusters that truly represent bulk behavior, since they provide statistical samples of bulk populations. Thus, the current study is aimed at revealing phenomena that result directly from the *collective* dynamics of SIA cluster ensembles.

It is shown here that when a fixed number of SIA clusters is introduced in the simulation box, and then the clusters are allowed to move both by random and drift motion under the influence of the force field of an edge dislocation, a substantial fraction of them ends up in a defect cloud that decorates the dislocation. A significant portion of SIA clusters are found to be trapped on the tensile side of the edge dislocation (between planes with normals of ±20° and ±40° with respect to the slip plane normal). The remaining fraction of SIA clusters is self-trapped in the matrix. Although SIA clusters can change their Burgers vector thermally with an activation energy that we assumed to be 0.05 eV per crowdion [8], the influence of the elastic field of existing dislocations is much more important in re-orienting clusters as they approach the dislocation [4]. Thus, SIA clusters drift towards the dislocation core trying to reach its tensile side, but in the process get self-trapped by their own mutual stress field. As a consequence, random events away from the dislocation core lead to the formation of self-trapped rafts, while those clusters that manage to come close to the dislocation participate in the formation of a decoration cloud, in line with earlier predictions by Trinkaus et al. [4]. The details of the SIA cloud build-up revealed here indicate that the majority of clusters, especially those close to the top of the cloud near the dislocation, are forced to re-orient their Burgers vector and align themselves in the direction of the dislocation's Burgers vector. Thus, the dislocation can be viewed as a strong source of polarization imposed on SIA clusters in the cloud. However, as the cloud builds up in the pyramidical shape consistent with the geometric expansion of the dislocation's stress field, new arrivals to the bottom of the cloud pyramid are shielded from the dislocation's field, and are self-trapped by clusters in adjacent layers.

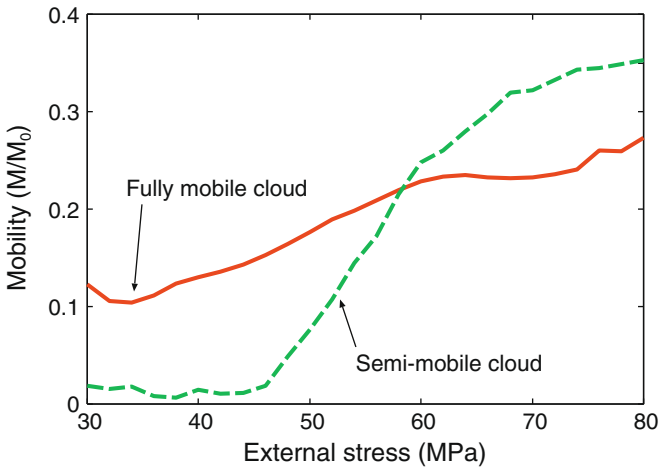

Fig. 13. Dislocation mobility M, normalized to the mobility M_0 in unirradiated crystal, versus applied resolved shear stress. Dashed line is for a cloud with a fraction of sessile clusters, and solid line is for a cloud with all mobile clusters.

Our simulations indicate that the build-up speed of SIA clouds is very fast, reaching quasi-equilibrium configurations within 5–20 ns. Thus, simulation of continuous irradiation is essentially equivalent to introduction of SIA cluster increments in the simulation volume that correspond to displacement damage dose increments, and then allowing them to reach their quasi-equilibrium before the next dose increment is added. Simulation results can thus be considered to approximate continuous irradiation if one accounts for the effect of recombination between SIA clusters and nano-size voids that also form in irradiated Fe. One poignant consequence of the saturation behavior in the kinetics of SIA cluster attachment to dislocation clouds is pointing out the need to modify the concept of dislocation bias that is a cornerstone of the rate theory of void swelling [28,29]. In the rate theory formalism, it is assumed that all dislocations have the same bias factor for absorption of interstitials, regardless of the irradiation dose. The present simulations demonstrate that the rate of absorption of SIAs into the dislocation core is limited by the build-up of its surrounding cloud, and that once the cloud forms; it partially neutralizes the dislocation field. Therefore, one is led to conclude that the dislocation bias towards interstitials is only transient if the dislocation does not move away from its surrounding cloud. The process of shielding of dislocations by SIA clouds parallels the concept of Debye shielding in electromagnetics, where in a plasma environment, electrons flow preferentially to positively charged poles to neutralize their influence on the bulk of the plasma. The spatial extent of the cloud may be regarded to be similar to the Debye shielding length in plasma.

The details of dislocation interaction with SIA ensembles reveal a few interesting features that are not captured by MD simulations of dislocation interaction with single SIA clusters. When the dislocation is pinned by a continuous cloud along the length of its core, it first develops small perturbations near weak points in the cloud, and then unzips away from the cloud at the critical shear stress. Since the attractive force of the cloud increases slowly with the irradiation dose (or cloud SIA content), it is expected that the CSS increases rapidly with dose early on during irradiation, then more slowly as irradiation proceeds. Once the dislocation is freed from its own cloud, it may encounter other cloud pockets that represent localized resistance to its further motion. Simulations of dislocation interaction with both static and dynamic clouds reveal that the general behavior is essentially the same, and that it resembles the interaction of a dislocation with a penetrable obstacle, such as a precipitate, void or bubble. As the dislocation approaches the cloud, some SIA clusters may re-arrange their configuration, but the majorities are locked into their self-trapped positions. The dislocation must therefore bend around the cloud obstacle, and in the process, will drag a few SIA clusters along their glide cylinders. Such dragged clusters slowly down dislocation motion once it achieves a critical curved configuration that allows it to be freed

from the collective SIA cluster field. If the applied stress is high enough, the dislocation may shed SIA clusters behind and achieve a higher speed as it is no longer resisted by the clusters.

In unirradiated materials, the yield point in a tensile test is reached when the applied stress is high enough to activate a significant population of F–R sources. However, further increase in plastic strain is governed by work-hardening, due to collective dislocation–dislocation interaction mechanisms. The situation is more complex in irradiated materials. The onset of plastic yield is a combination of F–R source activation and dislocation unlocking from SIA cluster atmospheres (source hardening). At low irradiation dose, F–R source activation is expected to dominate, but as the dose increases, source hardening will control the onset of plastic yield. The agreement between the present model of hardening by SIA clusters and experiments is qualitative because it ignores contributions to yield from activated F–R sources. Nevertheless, the magnitude of radiation hardening due to SIA clusters is more in agreement with experiments at high dose, indicating that the majority of dislocations are locked by their SIA clouds, and that yield is controlled by their release from clouds. The development of post-yield plastic flow is more complex, because it entails dislocation interaction with SIA clouds, nano-voids, precipitates in addition to normal work-hardening. Thus, although the present model of hardening captures the major contributions to the onset of plastic yield, it is not sufficient for post-yield behavior. Large-scale dislocation dynamics and crystal plasticity finite element methods may provide future opportunities to model post-yield plasticity of irradiated materials.

Acknowledgments

The present work was supported by the US Department of Energy (DOE), Office of Fusion Energy Sciences (OFES) through Grant DE-FG02-03ER54708, and the Office of Nuclear Energy through Grant DE-FC07-06ID14748 with UCLA. The authors would like to acknowledge discussions with Dr B. Singh during the course of this work.

References

[1] T.D. de la Rubia, M.W. Guinan, Phys. Rev. Lett. 66 (1991) 2766.
[2] H. Trinkaus, B. Singh, S. Golubov, J. Nucl. Mater. 283–287 (2000) 89.
[3] B.N. Singh, A.J.E. Foreman, H. Trinkaus, J. Nucl. Mater. 249 (1997) 103.
[4] H. Trinkaus, B.N. Singh, A.J.E. Foreman, J. Nucl. Mater. 249 (1997) 91.
[5] Y.N. Osetsky, D.J. Bacon, A. Serra, B.N. Singh, S.I. Golubov, J. Nucl. Mater. 276 (2000) 65.
[6] Y.N. Osetsky, A. Serra, V. Priego, J. Nucl. Mater. 276 (2000) 202.
[7] D. Rodney, G. Martin, Phys. Rev. B 61 (2000) 8714.
[8] M. Wen, N.M. Ghoniem, B.N. Singh, Philos. Mag. 85 (2005) 2561.
[9] E. Orowan, in: Symposium on Internal Stresses in Metals and Alloys, Institute of Metals, London, 1948, p. 451.
[10] A.K. Seeger, in: Proceedings of the Second United Nations International Conference on the Peaceful Uses of Atomic Energy, vol. 6, Geneva, 1958, p. 250.
[11] J. Friedel, Dislocations, Addison-Wesley, Cambridge, MA, 1964.
[12] F. Kroupa, P.B. Hirsch, Discuss. Faraday Soc. 38 (1964) 49.
[13] A.H. Cottrell, Dislocations and Plastic Flow in Crystals, Oxford University, London, 1953.
[14] C.C. Fu, J.D. Torre, F. Willaime, J.-L. Bocquet, A. Barbu, Nature Mater. 4 (2005) 68.
[15] J. Marian, B.D. Wirth, J.M. Perlado, Phys. Rev. Lett. 88 (2002) 255507.
[16] T.M. Robinson, Phys. Status Solidi A 75 (1983) 243.
[17] N.M. Ghoniem, L.Z. Sun, Phys. Rev. B 60 (1999) 128.
[18] D.J. Bacon, Y.N. Osetsky, R. Stoller, R.E. Voskoboinikov, J. Nucl. Mater. 323 (2003) 152.
[19] F. Gao, H. Heinisch, R.J. Kurtz, Y.N. Osetsky, R.G. Hoagland, Philos. Mag. 85 (2005) 619.
[20] F. Gao, G. Henkelman, W.L. Weber, L.R. Corrales, H. Jonsson, Nucl. Instrum. and Meth. B 202 (2003) 1.
[21] M. Eldrup, B.N. Singh, S.J. Zinkle, T.S. Byun, K. Farrell, J. Nucl. Mater. 307–311 (2002) 912.
[22] H. Trinkaus, B.N. Singh, A.J.E. Foreman, J. Nucl. Mater. 251 (1997) 172.
[23] N.M. Ghoniem, S.-H. Tong, L.Z. Sun, Phys. Rev. B 61 (2000) 913.
[24] F. Kroupa, Dislocation loops, in: B. Gruber (Ed.), Theory of Crystal Defects, Academic Press, New York, 1966, p. 275.
[25] R.E. Stoller, Z.J. Zinkle, J. Nucl. Mater. 349–352 (2000) 283.
[26] M. Makin, Philos. Mag. 10 (1964) 695.
[27] Z. Rong, Y.N. Osetsky, D.J. Bacon, Philos. Mag. 85 (2005) 1473.
[28] R. Bullough, B. Eyre, K. Krishan, Proc. R. Soc. London A 346 (1975) 81.
[29] N.M. Ghoniem, G.L. Kulcinski, Radiat. Eff. 41 (1979) 81.